Artisanal Lime Coatings and Their Influence on Moisture Transport During Drying

T. Diaz Gonçalves and V. Brito

Abstract Lime coatings such as whitewashes were originally used in historical buildings all across Europe and the rest of the globe, on lime plasters or directly on stone elements. Today, these coatings are increasingly used in conservation not only due to their unique aesthetic features but also for functional reasons. One of their main functional advantages is the ability to not hamper the drying of the substrate, which is very important because dampness is recurrent in historical buildings. The work presented here is aimed at improving the understanding of how and why lime coatings affect (or not) the drying of the porous building materials that usually constitute those substrates. We analysed experimentally the influence of one selected lime coating on the drying of five substrate materials with architectural relevance: one lime mortar and four stones, the well-known Ança limestone, Maastricht limestone and Bentheimer sandstone, as well as a common Portuguese low porosity limestone. All the materials were characterized in relation to their capillary porosity and pore size distribution. Afterwards, the drying kinetics of the substrate materials, when coated or uncoated, was evaluated and compared. It was concluded that the lime coating not only does not hinder drying, but can even accelerate it. Indeed, at high moisture contents, the drying rate increases up to as much as 50%. This is likely to happen because the coating generates a larger effective surface of evaporation. In the article, we discuss the possible causes and implications of this phenomenon.

Keywords Lime coatings · Porous materials · Drying · Moisture transport Historical buildings

T. Diaz Gonçalves (✉) · V. Brito
National Laboratory for Civil Engineering (LNEC), Lisbon, Portugal
e-mail: teresag@lnec.pt

V. Brito
e-mail: vbrito@lnec.pt

1   Introduction

Lime coatings are common in historical buildings all across Europe and elsewhere. They were originally used for aesthetical and sanitary purposes, and also to protect the substrates. Numerous variations of composition and texture can be observed, in interiors and exteriors, over lime plasters or, in some cases, directly on stone elements (Holmes and Wingate 1997). Limewashes are the most typical of these coatings (Fig. 1, on the left). They were obtained from aqueous suspensions of hydrated lime, sometimes including also pigments or additives, which were applied by brush. But thicker lime coatings were also frequent (Fig. 1, on the right). These were obtained from lime pastes and were applied by brush or with a spatula or similar tool.

After the industrial revolution, lime coatings were gradually replaced by synthetic coatings. These, however, eventually proved unsuitable for historic buildings. The reasons were aesthetic, because lime coatings have unique gloss and texture, but also functional. One of the most critical issues stems from the huge influence that coatings have in the drying of the underlying elements. Indeed, coatings are at the interface between the construction and its environment, thereby controlling all the exchanges of moisture between them. The presence of moisture is usual in historic constructions which are based on thick solid walls made of porous hydrophilic materials and built in direct contact with the ground. When coatings hamper the evaporation of this moisture, they can exacerbate moisture problems. This has often been observed when lime coatings are replaced by synthetic coatings. One typical problem is an increase in the height that water reaches in walls with rising damp. In these walls, water rises by capillarity up to where the liquid flow through the base of the wall is balanced by the vapour flow through its surfaces. Therefore, when this vapour flow is reduced, for example by a coating, the water has to climb higher in the wall to restore equilibrium.

To overcome these limitations of ordinary synthetic coatings, industrial coatings specific for application on old buildings have been developed. Today, there are several types of such coatings available on the market (Brito et al. 2011). They

Fig. 1 Whitewashed façade at Terena village, Alentejo, south Portugal (on the left) and a thicker lime coating on stone masonry at Rendufe Monastery, Braga, north Portugal (on the right)

usually seek to reproduce the aesthetical characteristics and functional advantages of traditional lime coatings, while presenting higher durability. One of main functional advantages is the ability to not impede the drying of the substrate, which the new industrial coatings seek to achieve by means of high vapour permeability. But is this high vapour permeability the only factor behind the good performance of traditional lime coatings?

To find the answer to this question and, in general, to better understand how and why traditional lime coatings affect (or not) the drying of porous building materials, we have analysed experimentally the influence of one selected lime coating on the drying of five different substrates. These five substrates include one lime mortar and four natural stones which are representative of those found in old buildings. Further, they all have different porosity and pore size distribution. In the following sections, we describe the methods used in this work and discuss the obtained results based on a comparison between the performance of coated and uncoated materials.

2 Materials and Methods

2.1 Substrates

The experimental work was conducted using small cubes with around 24 mm edge of the substrate materials described in Table 1, lime mortar and four types of natural stone. The lime mortar was prepared following standard EN 1015-2. Moulding and curing were carried out as described in Diaz Gonçalves et al. (2012), following as close as possible standard EN 1015-11. The stone cubes were cut from larger blocks.

The capillary porosity of the materials is given in Fig. 2. This was measured at atmospheric pressure, after 48 h complete immersion, following the procedure II.1 of RILEM (1980).

The main pore radius of the materials is also presented in Fig. 2. For the lime mortar and the two Portuguese stones, these values were obtained from the pore size distribution curves presented in Fig. 3. Pore size distribution was determined by mercury intrusion porosimetry (MIP) with an Autoscan60 instrument from Quantachrome, following ASTM D4404-84 (ASTM International 2004) and always

Table 1 Substrate materials

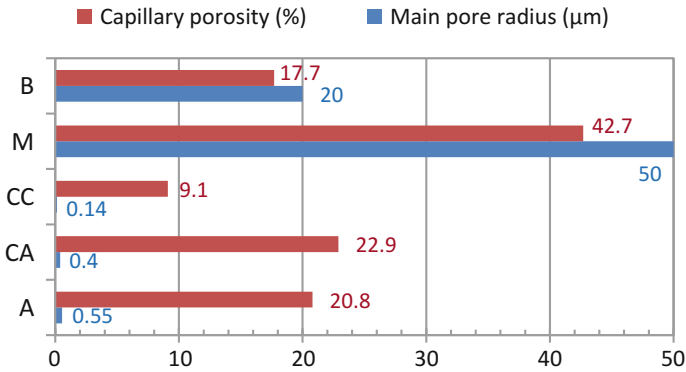| Ref.	Designation	Description
A	Lime mortar	Air lime:sand (1:3) mortar
CA	Ança limestone	Soft and porous stone from Coimbra, Portugal
CC	Grey limestone	Common Portuguese low porosity stone
M	Maastricht limestone	Light yellowish, soft and porous stone from the Netherlands
B	Bentheimer sandstone	Porous quartz-rich stone from Germany

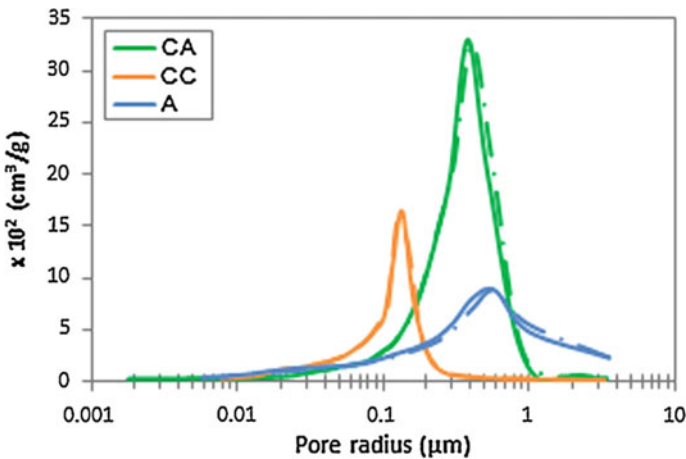**Fig. 2** Capillary porosity and main pore radius of the substrate materials

Fig. 3 Pore size distribution of the substrate materials

repeating the measurements. For the Bentheimer sandstone and Maastricht lime-stone, the main pore radius values reported by Dautriat et al. (2009) and De Clercq et al. (2007), respectively, are used. As seen, these two stones have much large pores.

The four lateral faces of the lime mortar and stone cubes were sealed with an epoxy resin. Afterwards, they were cleaned in a Branson 1200 ultra-sound cleaner.

2.2 Lime Coating

The lime coating was obtained by blending hydrated commercial lime powder (Lusical H100) with water. This lime is composed of calcium hydroxide $Ca(OH)_2$,

with no additives. A laboratory mixer of the type defined in EN 196-1 was used for that purpose. The lime was first mixed with water during 60 s at low speed, which was followed by manual incorporation of the material that adhered to the inner walls and, finally, by another 30 s mixing at the same speed.

The W/L ratio of the lime coating was established based on two main criteria: (i) maximization of the capillary porosity of the hardened paste; (ii) reasonable workability of the fresh paste. Five different W/L ratios were initially tested, 1.0, 1.2, 1.4, 1.6 and 1.8.

To evaluate the porosity of these five lime pastes, cubic specimens with 2.4 mm edge were moulded. They spent the first seven days in a conditioned room at 50% RH and 20 °C (in the first day inside a polyethylene bag), after which period they were demoulded and spent another fifteen days in a carbonation chamber at 21 °C, 65% RH and 5% CO_2. The capillary porosity was estimated as the percent ratio 100 V_w/V_s, where V_w is the volume of water absorbed after 48 h in partial immersion, and V_s the volume of the specimens. This volume was measured geometrically with a digital slide caliper. RILEM procedure II.1 of hydrostatic weighing could not be followed because the lime cubes disintegrated when totally immersed in water during 48 h. The pore size distribution was determined by MIP.

The capillary porosity of the hardened pastes has an inverted parabolic relationship with the W/L ratio (Fig. 4). This means that porosity increases up to certain percentage of mixing water. However, as we keep adding more water, it will eventually start decreasing. The reasons for this decrease are not totally clear and deserve further research. The increase in the W/L ratio involves also an initial increase of the main pore diameter, followed by stabilization (Fig. 5).

The initial increase of the capillary porosity with the W/L ratio is consistent with the results of Arandigoyen et al. (2005). However, their shorter range of W/L ratio does not allow detecting any further decrease in the capillary porosity, although a stabilization is devised at the higher W/L ratios.

Trial applications were then carried out to evaluate the workability of the pastes when applied as coatings. For W/L bellow 1.4, the lime pastes became very dry and
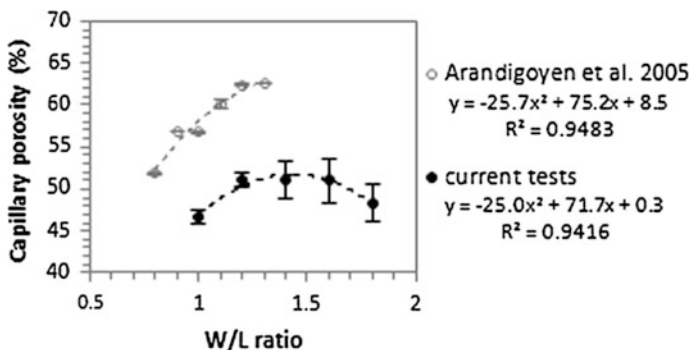

Fig. 4 Variation of the capillary porosity of the hardened lime pastes with their W/L ratio
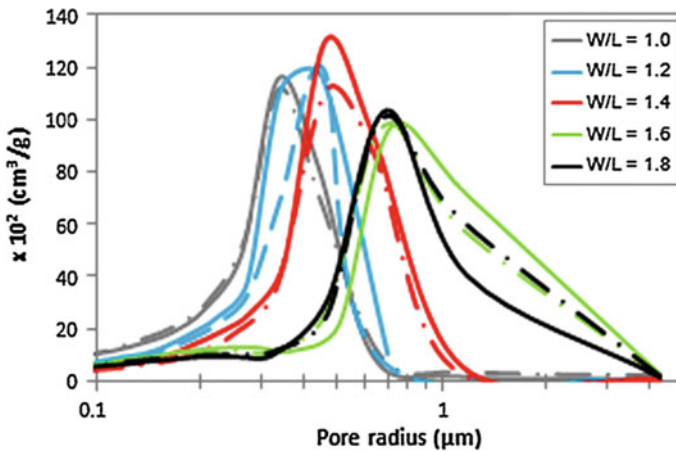
Fig. 5 Pore size distribution of the hardened lime pastes

a reasonable workability was not achieved. The lime paste with W/L = 1.4 was selected. Note that the porosity of the cubes should be considered only as a reference because the suction of the substrate may change it, and this change can be different for different substrate materials.

The lime coating was applied on mortar A using a paint-brush and on the remaining substrates using a spatula. The two different application techniques were necessary due to the different workability that the paste revealed on different substrates: workability was higher when the coating was applied on lime mortar substrate. Figure 6 shows that the consumption too varied with the substrate material. This means that the thickness of the coating may have changed too. However, no significant differences were visually noticeable.

2.3 Experimental Methods

The drying kinetics of the coated and uncoated substrate materials was evaluated by RILEM procedure II.5 (RILEM 1980). This procedure consists in saturating the specimens and then letting them dry through their top face, under controlled environmental conditions, while the loss of water is monitored by periodical weighing.

The specimens were oven dried at 40 °C until constant mass and placed in partial immersion in pure water for three days. Then, their bottom surface was sealed with polyethylene film. Drying took place in a conditioned room at 20 °C and 50% RH (Fig. 7). A minimum of four specimens of each kind was always used.

The results are expressed by the so-called evaporation curve (Fig. 8) whose slope corresponds to the drying rate. This curve is typically composed of two parts:
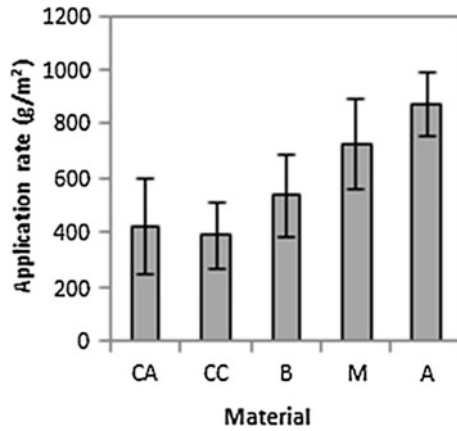
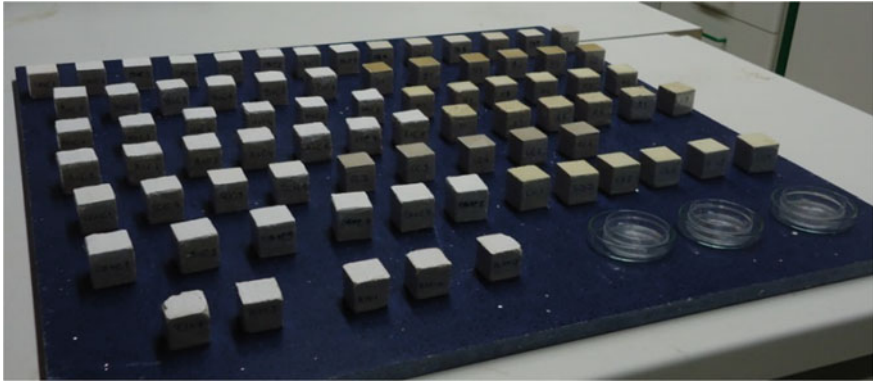**Fig. 6** Consumption of the lime coating on the five substrates

Fig. 7 Test set-up showing the 24 mm-edge specimens drying in the conditioned room, as well as water-filled petri dishes which were used to measure the evaporation rate of free water surfaces
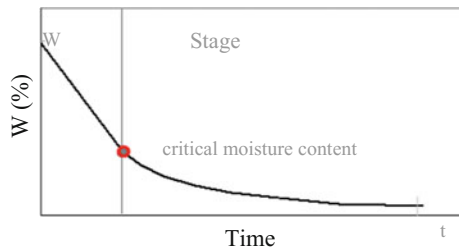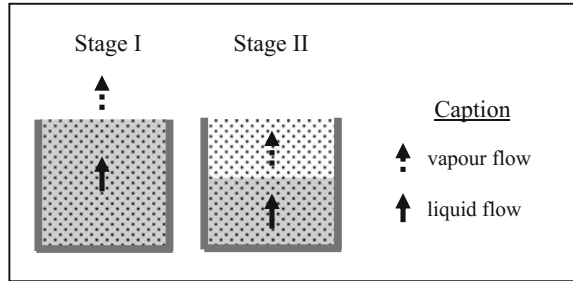
Fig. 8 Typical evaporation curve

Fig. 9 Two main drying
stages

an initial straight line segment, followed by a concave branch. The two parts
correspond roughly to the two main stages that a porous material undergoes when
drying from saturation (Fig. 9). Stage I, also called the constant drying rate period,
occurs while the moisture content is high enough to sustain a saturated condition at
the surface. Stage II, also called the falling drying rate period, starts when this
moisture content is no longer sufficient to produce a liquid flow able to compensate
the evaporative demand. In this second stage, the evaporation front recedes pro-
gressively into the material to maintain equilibrium between the liquid and vapour
flows. The drying rate decreases accordingly, with reduction of the vapour pressure
at the front and with the increase in the thickness of the dry layer that vapour has to
traverse to reach the outer surface.

When there are several specimens of each kind involved, as it is the case here,
the drying curve is not an appropriate way of expressing the results because there is
necessity of a statistical treatment of those results. In these cases, it is better to use
the drying index (*DI*), an empirical quantity that translates the drying curve into a
single quantitative parameter (Eq. 1):

$$DI = \frac{\int_{t_o}^{t_i} f(w_i) \times dt}{w_0 \times t_i} \tag{1}$$

f(wᵢ) is the mathematical expression of the drying curve, given as a function of
the moisture w_i (%), w_0 the water content at the beginning of drying and t_i (h) the
total duration of the test. Note that the slower the drying the higher the DI.

Specimens of the hardened lime paste (PC) were always tested to serve as refer-
ence. The evaporation rate of free water surfaces was also measured during the tests,
by the method described in Diaz Gonçalves et al. (2012), using full Petri dishes.

3   Results

The moisture content at the beginning of drying is not relevantly affected by the
lime coating, as seen in Fig. 10. This means that the comparisons between coated
and uncoated materials are free from distortions due to differences in the initial
moisture content of the specimens.

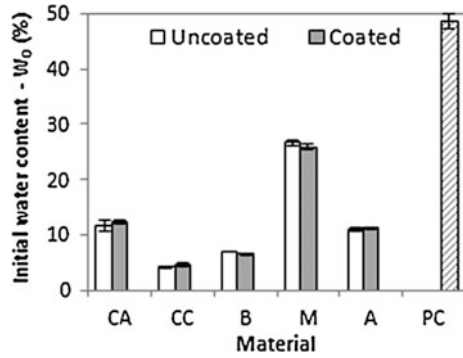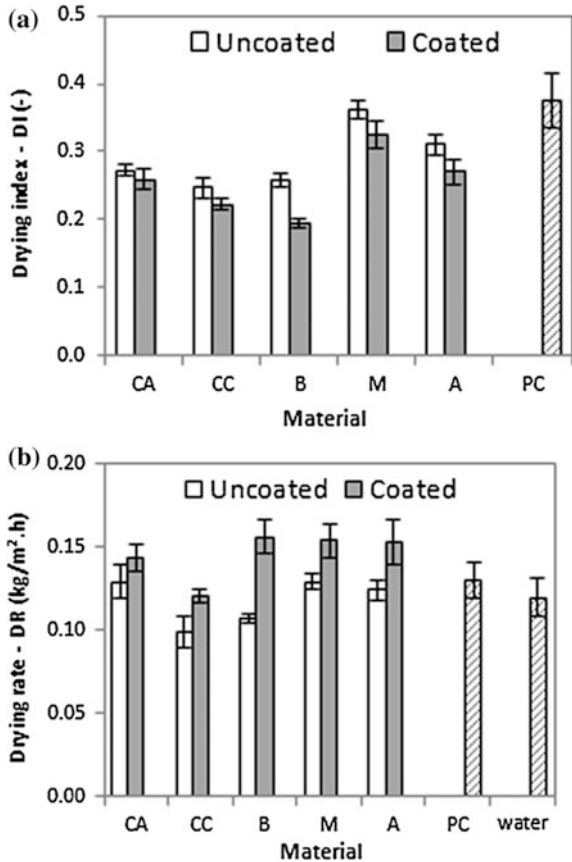**Fig. 10** Initial moisture content of the coated and uncoated materials and of the hardened lime paste

Fig. 11 Results of the drying test for the coated and uncoated materials, hardened lime paste and free water surface, in terms of **a** drying index and **b** stage I drying rate

The results of the drying test are given in Fig. 11 in terms of drying index and stage I drying rate. These results show that:

- The lime coating does not hinder the drying of the tested substrates. Strikingly, it even accelerates the process. This is clear both in terms of drying index (Fig. 11a) and, particularly, of the stage I drying rate (Fig. 11b). The greatest differences occur for the Bentheimer sandstone (B), whose drying index was reduced by 25% and stage I drying rate increased by 46%, respectively.
- The stage I drying rate is neither identical among the coated materials, nor between those and the hardened lime paste (Fig. 11b). This is contrary to what would be expected during a period where the evaporation front is always located at the surface, if the lime coating had always similar characteristics. It confirms, therefore, that substrates are able to change significantly the physical characteristics of the lime coating during its application and cure. This is in line with previous research results, for example, with those obtained within EU project COMPASS (EVK-CT 2001-00047).
- The drying rate of the materials, regardless of whether they are coated or uncoated, exceeds in several cases that of the free water surface (Fig. 11b).

4   Discussion

An overall acceleration of drying was observed for the five tested substrates after application of the lime coating (Fig. 11a). This overall acceleration can be due to the rise in the stage I drying rate (Fig. 11b). But why has this rate increased?

The reason is not obviously a high vapour permeability of the coating. That could justify, at the maximum, a drying rate as high as that of the uncoated substrate. Further, there is significant change of the stage I drying rate, and during this stage there is no vapour transport across the material because the wet front is at the surface.

It is, indeed, reasonable to assume that during stage I the wet front was at the surface of the specimens, either they were coated or not. This assumption would be unreasonable for a hydrophobic coating or one with larger pores than the substrate. Such coatings would be unable to absorb water from the substrate and, thus, the wet front would be located at the interface between the coating and the substrate (Petković et al. 2007). But our coating is hydrophilic and has pores within the range or smaller than those of the substrates. Indeed, this is the case with the lime paste cubes (Figs. 2, 3 and 5) and the suction of the substrate could, at the most, make these pores even smaller. So, we can safely admit that the wet front was at the surface during stage I.

A likely explanation for the higher drying rate that arises after application of the lime coating is that this coating increases the effective surface of evaporation, i.e., the dimension of the evaporating surface during stage I. Indeed, during this stage, the evaporation rate depends on the environmental conditions but also on the effective dimension of the evaporating surface. A larger effective evaporating surface obviously implies a higher drying rate for the material.

The effective surface of evaporation depends on the porosity of the material but also on other physical characteristics, such as the pore size distribution. The complex pore size distribution of the type of materials studied here gives rise to evaporating surfaces with irregular morphology, whose area may greatly exceed that of the projected surface. This explains also why the drying rate of the materials is, in some cases, even higher than that of a free water surface (Hammecker 1993; Jeannette 1997; Rousset-Tournier 2001; Diaz Gonçalves et al. 2012, 2014).

It is also interesting that the stage I drying rate of the lime coated materials is greater than that of the hardened lime paste itself (Fig. 11b). Indeed, all the coated materials were expected to have a drying rate very close to that of the hardened lime paste, because during stage I the drying front is located at the surface and this surface is always covered with the same lime paste. But Fig. 11b shows that this is not true. A first explanation is that each substrate is able to change, in a different way, the physical characteristics of the coating. The influence of the substrate could derive from the suction it exerts on the fresh coating. This suction varies with the capillary porosity and pore size distribution, and is probably also one of the factors behind the differences in workability (Sect. 2.2) and application rate (Fig. 6) observed among different substrates. A second explanation is that the transitional layer, where the coating interpenetrates the substrate, has also some effect in the stage I evaporation. This could occur because the menisci have to recede slightly into the material, so as to generate the capillary pressure gradient that drives the movement of liquid towards the surface. Since the coating is thin, the transitional layer could be reached by this small receding of the wet front.

The experimental results presented here suggest, therefore, that lime coatings are able to promote masonry drying in stage I conditions, i.e., at high moisture contents. High moisture contents can be found, for example at the base of walls with rising damp. Since the water rises up to where the evaporation flow through the surfaces balances the incoming liquid flow through the base of the wall, a faster stage I evaporation rate could allow reducing the height of capillary rise. It could also help reducing the temporal impact of moistening events, and eliminating the moisture trapped in a wall after the source is deactivated.

We think that this effect and the advantages that lime coatings thereby provide in terms of health conditions were probably intuited and experienced in practice by the ancient. Although the application of lime coatings on damp walls is problematic, the truth is that in most cases the moisture content of those walls has seasonal variations.

5   Conclusions

The main conclusion of this work is that the lime coating not only does not hinder drying, but can even accelerate it for a wide range of substrate materials. The acceleration in drying rate is particularly significant for stage I conditions, i.e., when the moisture content of the substrate is high enough so that the wet front is located

at the surface, as it often happens at the base of walls with rising damp. This beneficial effect on the stage I drying rate is not due to a high vapour permeability of the lime coating. It may be explained by a high effective surface of evaporation arising from the geometric complexity of its pore structure. We think the advantages that lime coatings thereby provide in terms of health conditions were probably intuited and experienced in practice by the ancient.

The magnitude of the increase in the stage I drying rate varies with the type of substrate, and may reach values in the order of 50%. It would be important, in future work, to understand better the mechanisms behind this influence of the substrate.

References

Arandigoyen, M., Pérez Bernal, J. L., Bello López, M. A., & Alvarez, J. I. (2005). Lime-pastes with different kneading water: Pore structure and capillary porosity. *Applied Surface Science, 252,* 1449–1459.

ASTM International. (2004). Test method for determination of pore volume and pore volume distribution of soil and rock by mercury intrusion porosimetry. ASTM Standard D 4404-84.

Brito, V., Gonçalves, T. D., & Faria, P. (2011). Coatings applied on damp building substrates: Performance and influence on moisture transport. *Journal of Coatings Technology and Research, 8*(4), 513–525.

Dautriat, J., Gland, N., Guelard, J., Dimanov, A., & Raphanel, J. L. (2009). Axial and radial permeability evolutions of compressed sandstones: End effects and shear-band induced permeability anisotropy. *Pure and Applied Geophysics, 166*(5–7), 1037–1061.

De Clercq, H., De Zanche, S., & Biscontin, G. (2007). TEOS and time: the influence of application schedules on the effectiveness of ethyl silicate based consolidants. *Restoration of Buildings and Monuments an International Journal (Bauinstandsetzen und Baudenkmalpflege eine internationale Zeitschrift), 13*(5), 305–318.

Diaz Gonçalves, T., Brito, V., & Pel, L. (2012). Water vapour emission from rigid mesoporous materials during the constant drying rate period. *Drying Technology: An International Journal, 30*(5), 462–474.

Diaz Gonçalves, T., Brito, V., Vidigal, F., Matias, L., & Faria, P. (2014). Evaporation from porous building materials and its cooling potential. *Journal of Materials in Civil Engineering, 27*(8), 04014222.

Hammecker, C. (1993). *Importance des transfers d'eau dans la dégradation des pierres en oeuvre (Importance of water transfers in the degradation of stones in the site)*, Thèse de doctorat (Ph.D. thesis). Strasbourg, France: University Louis Pasteur.

Holmes, S., & Wingate, M. (1997). *Building with lime: A practical introduction*. London: Intermediate Technology Publications. ISBN 1853393843.

Jeannette, D. (1997). Structures de porosité, mécanismes de transfert des solutions et principales altérations des roches des monuments. In R. A. Lefèvre (Ed.), *La pietra dei monumenti in*

ambiente fisico e culturale (pp. 49–77). Ravello: European University Centre for Cultural Heritage.

Petković, J., Huinink, H. P., Pel, L., Kopinga, K., & van Hees, R. P. J. (2007). Salt transport in plaster/substrate layers. *Materials and Structures, 40*(5), 475–490.

RILEM TC 25-PEM. (1980). Recommended tests to measure the deterioration of stone and to assess the effectiveness of treatment methods, Test No. II.1 "Saturation coefficient", Test No. II.5 "Evaporation curve", *Materials and Structures*, *13*, 204–207.

Rousset-Tournier, B. (2001). *Transferts par capillarité et évaporation dans des roches. Rôle des structures de porosité (Capillary transport and evaporation in rocks. The role of pore structures)*, Thèse de doctorat (Ph.D. thesis), University Louis Pasteur, Strasbourg, France.